A project report on

Numerical analysis of hydraulic jump by an impinging jet

By

G HEMANTH RAGHAV

212ME3305

Under the supervision of

Dr. MANOJ K. MOHARANA

DEPARTMENT OF MECHANICAL ENGINEERING

NATIONAL INSTITUTE OF TECHNOLOGY ROURKELA

JUNE-2014

CERTIFICATE

This is to certify that the thesis entitled, "**NUMERICAL ANALYSIS OF HYDRAULIC JUMP BY AN IMPINGING JET**" submitted by Mr. G Hemanth Raghav in partial fulfilment of the requirements for the award of Master of Technology degree in Mechanical engineering with specialization in thermal engineering at the National Institute of Technology, Rourkela (deemed university) is an authentic work carried out by him under my supervision and guidance.

To the best of my knowledge, the matter embodied in the thesis has not been submitted to any other university or institute for the award of any degree or diploma.

Date:

Dr. Manoj K Moharana
Department of Mechanical Engineering
National Institute of Technology Rourkela
Rourkela 769008

SELF DECLARATION

I, Mr G Hemanth Raghav, Roll No. 212ME3305, student of M. Tech (2012-14), Thermal Engineering at Department of Mechanical Engineering, National Institute of Technology Rourkela do hereby declare that I have not adopted any kind of unfair means and carried out the research work reported in this thesis work ethically to the best of my knowledge. If adoption of any kind of unfair means is found in this thesis work at a later stage, then appropriate action can be taken against me including withdrawal of this thesis work.

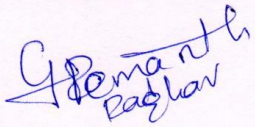

NIT Rourkela
02 June 2014

G Hemanth Raghav

Acknowledgement

I would like to thank and express my gratitude towards my supervisor Dr. Manoj K Moharana for his extensive support throughout this project work. I am greatly indebted to him for giving me the opportunity to work with him and for his belief in me during the hard times in the course of this work. His valuable suggestions and constant encouragement helped me to complete this master's thesis work successfully. It was a great experience to work under him given the amount of valuable knowledge gained. He has been a source of inspiration for me.

I would also like to thank the Department of Mechanical engineering for providing the CFD lab where the project work was done.

Place:

Date: G Hemanth Raghav

Abstract

This numerical work compares the available CFD transient models of an impinging jet under turbulent conditions. The rate of heat transfer into a water impinging jet on a hot flat aluminium plate was studied. The temperature of the plate was kept under the boiling point of water for analyzing the case without any phase changes. For computational purposes, we are studying the heat transfer due to a single 2D axisymmetric jet under different discharge rates in addition to predicting the location of the hydraulic jump and comparing it with different existing numerical correlations. The RANS model in ANSYS Fluent was used with the RNG k-ε with surface tension models and set level VOF methods, as it is best suited for our flow conditions. The boundary conditions used were under two cases, constant wall temperature and constant heat flux condition. Grid independence test techniques were also carried out. The results obtained for both the hydraulic jump and variation of Nusselt number as a function of Reynolds number through the simulation agreed consistently well with the existing results in literature with a maximum 6% deviation.

Keywords: potential core, hydraulic jump

Contents

List of Figures

Nomenclature:

g	Acceleration due to gravity, m/s^2
h	Heat transfer coefficient, W/m^2K
k_l	Thermal conductivity of liquid used, W/mK
Nu	Nusselt number
P	Pressure force, N/m^2
Pr	Prandtl number
q"	Heat flux in W/m^2
Q	Heat transfer, W
r	Radius, m
Re	Reynolds number
S	Source term
T_f	Temperature of fluid, ^oC
T_s	Temperature of surface material, ^oC
u	Velocity, m/s
	Greek symbols:
α	Phase fraction
ρ	Density, kg/m^3
ϑ	Kinematic viscosity, m^2/s
μ	Dynamic viscosity, Pa-sec

Chapter 1

Introduction

A run-out table is a kind of material handling device primarily designed to hold the tube after it has been cut to the required length and then transfers the heated tube to another holding area. The controlled cooling of steel strips on the run-out table is required to attain the high quality standards of flat-rolled steels used in many application oriented industries such as automotive applications, petroleum, chemical and construction. The run-out table is an essential part of the steel production line where the steel is being cooled from about 900 ^{o}C to 200 ^{o}C while the sheet is running at a certain speed. Due to the big temperature difference, modelling of boiling is important but due to the complexity involved in the mathematical modelling, we are not involving phase change. Hence the primary investigation in this thesis will be without considering phase changes.

Strict control of the high temperature of the strip during the various cooling techniques is of paramount importance as the rate of cooling affects the type of material characteristics required in the hot strip run-out is necessary, but very little success has been reached in this stage of optimization of the heat removal since no real practical understanding of the physical mechanisms involved have been recorded. The heat transfer behavior of the run-out table has been modelled in the investigation to quantify parameters affecting the final product quality of hot strip coil. Impingement of water at different angles with different type of nozzles with varying the rate of discharge, among them the liquid jet impingement perpendicular to the plate with circular nozzle are common because of their high mass and heat transfer rate and robustness.

As the experimental measurements of the local heat transfer coefficients may involve a highly complex process, the modeling of the cooling mechanisms is engineered to obtain the local thermal response of steel strips during their processing, hence requiring mathematical modeling to accurately predict the thermal and the micro-structural responses of the heated steel in process. Also this application is useful for V/STOL aerodynamics and freezing of tissues in cryosurgery.

The controlled cooling of steels on the run-out table has hence become a very commonly used practice in the production of hot rolled products in the steel industry. Also jet impinging in the micro-scale ranges is of paramount importance to model cooling of electronic chips and also in cooling of combustion of engines.

A number of experimental and theoretical studies have been conducted to understand the physics of heat transfer due to impinging jets either water or air over a flat plate at various angles, discharge rates and impinging materials.

CFD has been used in our investigation without involving phase changes to analyse a single liquid jet targeting a moving heated strip segmented portion. This cooling problem is then simplified to a jet impingement cooling of a heated strip. We investigate a 2D axisymmetric single jet model using RANS model in ANSYS FLUENT to understand the flow behavior and also to carry out the heat transfer analysis. Analytical observation shows that the water film near the wall was very thin almost down to a millimeter. To capture the free surface of the water, to preserve conservation and also to resolve the water film on the plate a very fine discrete mesh was required close to the wall where boundary layer effects are of paramount importance. In practice a run-out table consists of many jets, however in our study we have used a single jet for simplicity considering the large amount of mesh required.

Chapter 2

Physics of an impinging jet

Using impinging water jets is one of the most effectively efficient ways of heat transfer [1]. A well-directed liquid/ gaseous flow released against a surface can efficiently transfer large amounts of thermal energy between surface and fluid. Hence jet impingement is an effective way for cooling and is used in many applications because of its capacity to transfer very high heat fluxes by using the latent heat fluxes. When a liquid jet hits a wall surface, sudden increase in pressure occurs which then forces the liquid to accelerate from the stagnation points outwards in a thin liquid film of the order of a millimeter which covers the whole surface. The friction effect over the plate creates a kinematic boundary layer and the temperature difference between the liquid and the surface created a thermal boundary layer. The thermal and the momentum boundary layer thickness are determined by the underlying flow situations. The thickness of the film or the boundary layer is determined by the Reynolds number flow. The liquid film thickness can significantly vary for the laminar and the turbulent flow. The velocity of the liquid decreases with distance from the stagnation point and hence the liquid film and also the boundary layer gets thicker. The most important changes between flow regimes occurs within 5-8 jet diameter radial distance from the impinging point. This region is termed as potential core [2].

There are three distinct jet impingement configurations namely the free-surface jet, which uses dense liquid in a medium that is less dense such as air, secondly the submerged jet, which allows the fluid to impinge in the same fluid and thirdly, the confined submerged jet i.e., by confining the wall. The shape of the free surface is a critical factor of the gravitational force, pressure and surface tension. Also these forces depend on the shape, size and speed of the nozzle exit being used. In our analysis we will consider the free surface liquid jet.

Obtaining the heat transfer through jet impingement is a very complicated process involving numerous multiple factors such as the Reynolds number, prandtl number, jet diameter and wall to nozzle spacing.

As shown in the Schematic diagram Fig. 2.1, is the stagnation zone found perpendicular to the jet nozzle and after this stagnation region lies the radial flow zone. The width of the stagnation zone depends on the jet diameter, perpendicular distance between the nozzle and plate and the

Reynolds number. The most important phenomenon in the impinging of a jet is the characteristic feature of a hydraulic jump, which occurs due to the deceleration of the fluid. The location of the hydraulic jump was determined and compared by a correlation which will be discussed later.

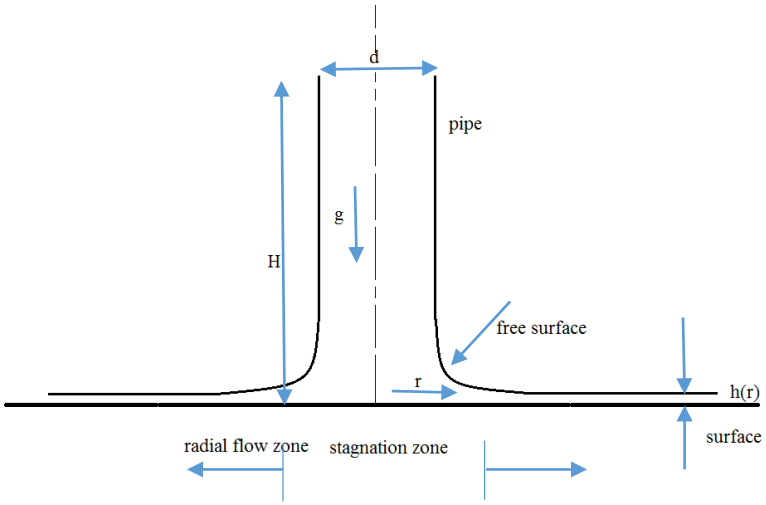

Fig. 2.1: Schematic diagram of an axisymmetric model [2]

There are three characteristic regions:

1) Free jet region
    i) Potential core
    ii) Shear layer
2) Impingement region or stagnation region
3) Wall jet region

The thin hydro-dynamic and thermal boundary layers within the stagnation point help remove a large amount of heat [3].

A circular liquid if impinging vertically on a horizontal surface produces a radially spreading film flow. If the flow rate is more than the critical, then the film is thin and the flow is supercritical a short distance away from the point of impingement; the film thickness is typically a fraction of a millimeter. A circular hydraulic jump may be formed at some distance. The parameters of the problem are the jet flow rate, the jet radius at the point of impingement, fluid kinematic viscosity and surface tension, acceleration due to gravity, the plate radius and the jet velocity related by

$$U_j = Q/\pi a^2 \qquad (1)$$

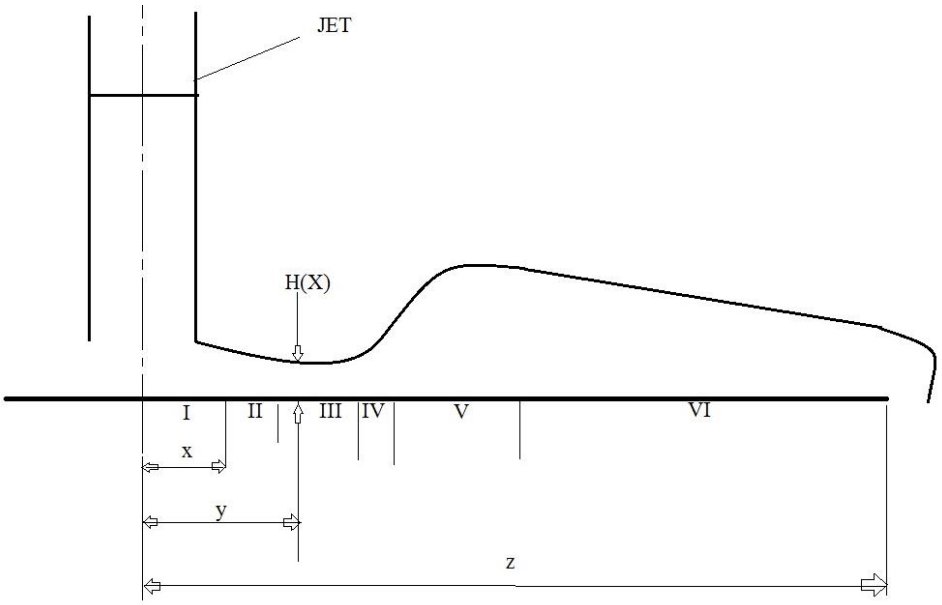

Fig. 2.2: Various regions in the radial flow [4].

(I) Stagnation region;

(II) Developing region where the boundary layer is below the free surface and the velocity above the boundary layer is approximately equal to the jet velocity.

(III) Developed region where viscous effects are felt up to the free surface and gravity is not important.

(IV) Gravity effects are important and an adverse pressure gradient is present.

(V) The hydraulic jump region including the separation eddy;

(VI) Flow downstream of the jump up to the edge of the plate z [4].

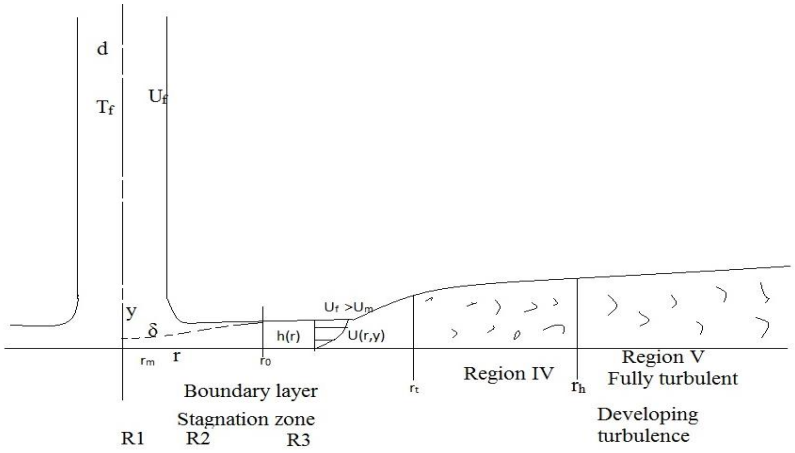

Fig. 2.3: Different zones of an axisymmetric impinging jet [3]

R1: The stagnation zone, R2: The laminar boundary layer where the momentum boundary layer is smaller than the liquid film thickness h(r), R3: The momentum boundary layer reaches the film surface, Region IV: This is the region from transition to turbulent where the momentum and the thermal boundary layer both reach the liquid surface, Region V: the flow is fully turbulent, T_f is fluid temperature, U_f is fluid velocity at inlet, U_m the free stream velocity, δ is the viscous boundary layer thickness, r_0 radius at which the viscous boundary layer reaches the free surface, r_t the radius at which turbulent transition begins and r_h is radius at which turbulence is fully developed [3].

Conservation Equations

The governing equations for fluid flow are governed by the continuity and the momentum equations namely the Navier-Stokes equation. The general form is [5]:

$$\frac{D\rho}{Dt} + \rho \frac{\partial u_i}{\partial x_i} = 0 \tag{2}$$

$$\rho\left(\frac{\partial u_i}{\partial t} + u_i \frac{\partial u_i}{\partial x_i} + u_j \frac{\partial u_i}{\partial x_j} \right) = -\frac{\partial p}{\partial x_i} + \mu \frac{\partial^2 u}{\partial x^2} + \rho F_i \tag{3}$$

$(\tau)_{ij}$ is the shear stress tensor, ρ is the intensive property density, u_i is the velocity, p is pressure, F_i is the force term and μ is the molecular viscosity. The summation convention is the one being used in the governing equations.

While considering incompressible flow studies, the density changes are assumed to be incompressible i.e. ρ = c, Eq. (2.1) reduces to the incompressible form [5]:

$$\frac{\partial u_i}{\partial x_i} = 0$$

$$\frac{\partial u_i}{\partial t} + u_j \frac{\partial u_i}{\partial x_j} = -\frac{1}{\rho} \frac{\partial p}{\partial x_i} + \upsilon \nabla^2 u_i + F_i \tag{6}$$

where, υ = μ/ρ is the kinematic viscosity. In the incompressible form of N-S equations, the momentum equation reduces to a divergence free constraint and using that the stress tensor term τ_{ij} in Eq. (3) is simplified to

$$\frac{\partial^2 u_i}{\partial x_j \partial x_j} = \nabla^2 u_i \tag{7}$$

Turbulence modelling:

The RANS based model is used for analysis of turbulent flow using commercially available ANSYS FLUENT®. The advantages of this model is that it takes lesser computational time than the large eddy scale simulation, discrete eddy simulation based models because these models consider only the time averaged properties and neglecting the instantaneous values. There velocity consists of two components such that

$$u = \bar{u} + u' \tag{8}$$

where $\bar{u}$ is the mean component and $u^{|}$ being the fluctuating component. The continuity and momentum equations are given by [6]:

$$\frac{\partial \rho}{\partial t} + \frac{\partial \left(\rho \bar{u}_i\right)}{\partial x_i} = 0 \tag{9}$$

$$\frac{\partial \left(\rho \bar{u}_i\right)}{\partial t} + \frac{\partial \left(\rho \bar{u}_i \bar{u}_j\right)}{\partial x_j} = -\frac{\partial \bar{p}}{\partial x_i} + \frac{\partial}{\partial x_j}\left[\mu\left(\frac{\partial \left(\bar{u}_i\right)}{\partial x_j} + \frac{\partial \left(\bar{u}_j\right)}{\partial x_i} - \frac{2}{3}\delta_{ij}\frac{\partial \left(\bar{u}_i\right)}{\partial x_i}\right)\right] + \frac{\partial \left(-\rho \bar{u}_i' \bar{u}_j'\right)}{\partial x_j} \tag{10}$$

The Reynolds stress term ($\rho\overline{u_\iota^{|} u_j^{|}}$) requires additional modeling to close the RANS equation hence the mathematical closure. The Boussinesq hypothesis can be used to relate the Reynolds stress to the mean velocity gradients as follows:

$$-\rho \bar{u}_i' \bar{u}_j' = \left[\mu_t\left(\frac{\partial \left(\bar{u}_i\right)}{\partial x_j} + \frac{\partial \left(\bar{u}_j\right)}{\partial x_i}\right) - \frac{2}{3}\left(\rho k + \mu_t \frac{\partial \left(\bar{u}_i\right)}{\partial x_i}\right)\delta_{ij}\right] \tag{11}$$

μ_t is the turbulent viscosity and k is the turbulent kinetic energy.

This modeling is available with k-Ɛ and k-ω in FLUENT which requires to solve another two transport equations, for example for turbulent kinetic energy k and Ɛ turbulent dissipation rate in the k- Ɛ model used for all our simulations as turbulence model. There are also several version of the k- Ɛ equations. We used the realizable k-Ɛ model since it predicts the spreading rate for axisymmetric as well as planar jets very well [6].

Convective heat transfer

In our analysis due to the involvement of heat transfer we have to consider the energy equation with the k- Ɛ model. The energy equation employed is [6]:

$$\frac{\partial \left(\rho E\right)}{\partial t} + \frac{\partial \left[u_i\left(E\rho + p\right)\right]}{\partial x_i} = \frac{\partial}{\partial x_j}\left(k_e \frac{\partial T}{\partial x_j} + u_i\left(\tau_{ij}\right)_{eff}\right) + s_h \tag{12}$$

where E is the total energy, T is temperature, k is thermal conductivity, $k_e = k + \frac{c_p \mu_t}{pr_t}$ the effective thermal conductivity, Pr_t is the turbulent Prandtl number, $(\tau_{ij})_{eff}$ is the deviatoric stress tensor and S_h is the source term.

In our convective heat transfer model for the impingement of the jet, the analyzed quantities are the heat transfer coefficient h, the non-dimensional form of heat transfer coefficient is the Nusselt number Nu, at the wall surface. The convective heat transfer coefficient is also calculated from the heat flux q" at the temperature constant wall surface given by the equation,

$$q'' = h\left(T_w - T_\infty\right) \tag{13}$$

where, T_w and T_∞ are the surface and free stream temperature respectively.

The local surface heat flux can further be obtained by using the Fourier law of heat conduction at the location of the boundary layer by the following equation,

$$q'' = -k_l \left.\frac{\partial T}{\partial y}\right|_{y=0} \tag{14}$$

The Nusselt number Nu_d based on the diameter of the nozzle can be calculated from the heat transfer coefficient h by,

$$Nu_d = \frac{hd}{k_l} \tag{15}$$

where d is the diameter of the jet nozzle and k_l is the heat conductivity of fluid.

Volume of Fluid method (VOF)

The impingement of water jet as a free surface flow captured by using the Volume of Fluid (VOF) method. This VOF method pioneered by Hirt and Nicholas [7].This method traces fluid regions through a eulerian mesh of stationary cells. It calculates the volume fraction of liquid in all the control volumes and depending on the value of the volume fraction it finds the cells that contain the interface. If the volume fraction α_r for phase r is zero, then it implies that the cell is empty and is the same when it shows one implying a free surface. In case it is between these two values then it implies an interface. The set-level method is used. The VOF-equation that is solved in VOF model is [10] as shown in Eq. (16). In addition to VOF we have used the surface tension model resulting in a source term in momentum equation [10].

$$\frac{1}{\rho r}\left[\frac{\partial(\alpha_r \rho_r)}{\rho_t} + \nabla.\left(\alpha_r \rho_r \vec{v}\right) = S_{\alpha r} + \sum_{p=1}^{n}\left(\dot{m}_{pr} - \dot{m}_{rp}\right)\right] \quad (16)$$

$\dot{m}_{pr}$ is the mass transfer from p to r phase.

$\dot{m}_{rp}$ is the mass transfer from phase r to phase p.

$S_{\alpha r}$ is source term and ρ_r is the density for phase r.

Chapter 3

Literature Review

We find many theoretical and experimental and experimental work in this research area of an impinging jet on a flat surface but numerical simulations are far too less. Hence the need to look into the analytical and experimental work by various authors.

In the study of heat transfer the Nusselt number has a direct measure on the heat transfer coefficient; hence a study on the number is of prime importance. At the stagnation point the nusselt number has been described as a function of Reynolds number and the Prandtl number by some of the authors as

$$Nu_0 = C\, Pr^m\, Re^n \tag{17}$$

By fitting in the values of C, m and n to the analytical solution of the boundary layer equations. Outside the stagnation region the nusselt number correlations are thoroughly investigated but for laminar flows whereas not for turbulent flows, in which case different authors have summarized the results. Turbulent heat transfer being more complicated than laminar cases.

The two types of boundary conditions used mainly in heat transfer are, the constant heat flux and the constant temperature at the wall surface. We are considering a constant temperature heat transfer condition such that the water does not reach the boiling point throughout the surface.

Fujimoto et al. [8] numerically studied free surface impinging jet on the convective heat transfer to a radial free surface jet impinging on a hot solid-using RIPPLE CFD code but important as stagnation zone this study is done without considering turbulence without hydraulic jump.

Craik et al. [9] analysed circular hydraulic jump formed on a circular horizontal steel plate when struck by a vertical jet of water. Newly conducted observations of this phenomenon are discussed here in detail. The most important observation is of an unreported instability of the jump which is examined here importantly and showing a rise when the local Reynolds number just ahead of the jump crosses a critical value of 147. Studies previous to this suggest that this instability is caused due to the flow behind the jump as it contains a closed eddy, the length of the eddy which decreases to zero as it increases towards its aforementioned critical value. The physical explanations of this flow structure and instability are proposed in this paper.

Lienhard et al. [3] studies the several aspects of liquid jet impingement cooling and focuses on the research that is being done at their laboratory. Free surface and circular hydraulic jump are

considered. Theoretical and experimental results for the laminar stagnation zone are summarized. Turbulence effects are also discussed.

Zuckermann and Lior [10] studied the physical mechanisms by which multiple peaks occur in the transfer coefficients profiles, and clarify which mechanism dominates various geometries and Reynolds number regimes. Develop a turbulence model and associated wall treatment if necessary, that reliably and efficiently provides time-averaged transfer coefficients. Given that the varied and inaccurate results of the alternatives, the SST and V2f models offer best results for less computational time.

Passandideh et al. [11] investigated the increasing of flow rate or decreasing the liquid velocity leading to a larger jump. When the height of the downstream is increased further, the radius of the circular hydraulic jump also decreases up to a certain limit. If the value of gravity is further increased, the radius of the circular hydraulic jump and the length of the included transition zone will be simultaneously increased, meaning which the circular hydraulic jump being bigger in low gravity than normal gravity conditions eventually. The radius of circular hydraulic jump in microgravity conditions shows lesser sensitivity to the downstream height than with its value in normal gravity.

Kasimov [12] provided the theory of steady circular hydraulic jump modeled on the principle of shallow-water model which is derived from the depth-averaged Navier-Stokes equations. The fluid flow structure upstream of the jump and downstream of jump is calculated by considering the flow over a flat circular plate of a finite radius. The radius of the circular hydraulic jump is determined using far-field boundary conditions coupled with the jump conditions which involves effects of surface tension. It is shown here that a steady circular hydraulic jump will not exist if surface tension is above a certain critical limit. The theoretical solution of the problem provides a basis for the hydrodynamic stability of the circular hydraulic jump.

Bush et al. [13] experimentally studied striking flow structures that are caused due to the effect of a vertical jet of fluid impinging on a thin fluid layer on a horizontal boundary. Also demonstrated were polygonal forms of polygonal jumps and a clear case of an independent study of a steady asymmetric jump that forms in various shapes. A parametric study shows the strong dependence of the jump structure on the principle governing dimensionless groups as the symmetry breaking responsible for the asymmetric jumps is interpreted as resulting from a capillary instability of the circular jump.

Kate et al. [14] investigated circular hydraulic jump formed on a flat plate due to a perpendicular impinging jet as it changes its shape when the jet inclination angle is varied through 90 degrees. Jumps formed when inclination angles ranges between 0 and 90 degrees is elliptic. Hydraulic jumps with corners are importantly observed when jet inclination angle change is less than or equal to the critical value. The formation of corners, in these jumps is predominantly due to the jump and jet interaction and jump to jump interaction at the lower jet inclination angles. Mainly the thin liquid film area bounded by the jump increases as the jet inclination angle increases by being maximum when the jet impinges perpendicular to the horizontal plate. In case of the inclined jets the considerable variations in the liquid film thickness in azimuthal direction is observed.

Chapter 4

Computational Domain

2D-Axisymmetric Model:

In CFD, newly developed turbulence models are applied to the generic, already established cases to evaluate and validate their performance. Many a times the models are simplified from their practical case such as the current study by assuming a 2D geometry and an axisymmetric condition. This may not work well for real world problems but if the trends are correct then it is still of industrial interests. Hence the use of the current RNG k-Ɛ model. The commercial package used was ANSYS FLUENT®. The domain was simplified and made as small as possible to minimize the mesh elements. Fig. 4.1 depicts the geometry which has been solved for a 2D axisymmetric case.

In this chapter the results of the 2D axisymmetric model, single jet are being presented. Later the results of the axisymmetric model are compared with the analytical solutions available from the literature. For the 2D axisymmetric model seven simulations are performed with a constant temperature. For the single jet 2D jet model, a constant temperature of 100 degree Celsius with a water speed of 5 m/s at the inlet at the maximum.

According to Zuckerman and Lior [19], the use of jet devices for heat transfer are described and with main focus on the numerous cooling applications. Hence a numerical simulation techniques and results are discussed herein with the pros and cons of all the available turbulence models available in FLUENT® and are compared for heat transfer for select models only by quantitative assessments of model errors and judgments of model requirability. According to the study RNG K-Ɛ is suitable for our computational purpose.

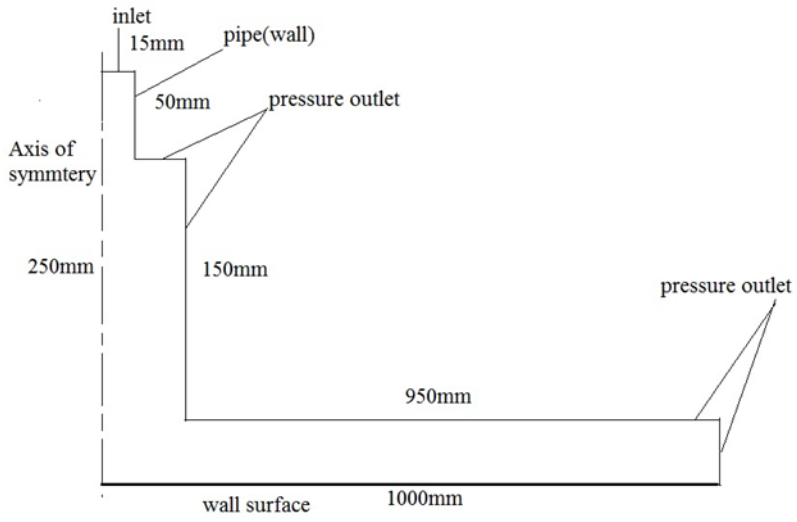

Fig. 4.1: A schematic representation of computational domain

Fig. 4.2: Geometry created in design modeler

The orthogonally of the meshed elements were of value 1 implying perfectness. A highly refined mesh was provided near the boundary to capture the interface and also the thermal and fluid effects in the boundary layer. The mesh quality is also tabulated.

Table 1: Mesh quality parameters

Type	Elements	Mesh used	Max aspect ratio	Min orthogonal quality
Mesh_70	61600	quadrilateral	1.7733	1.25
Mesh_90	77600	quadrilateral	2.28	1.25
Mesh_95	81600	quadrilateral	2.4067	1.25
Mesh_100	85600	quadrilateral	2.5333	1.25

Fig. 4.3: Computational Mesh of Model

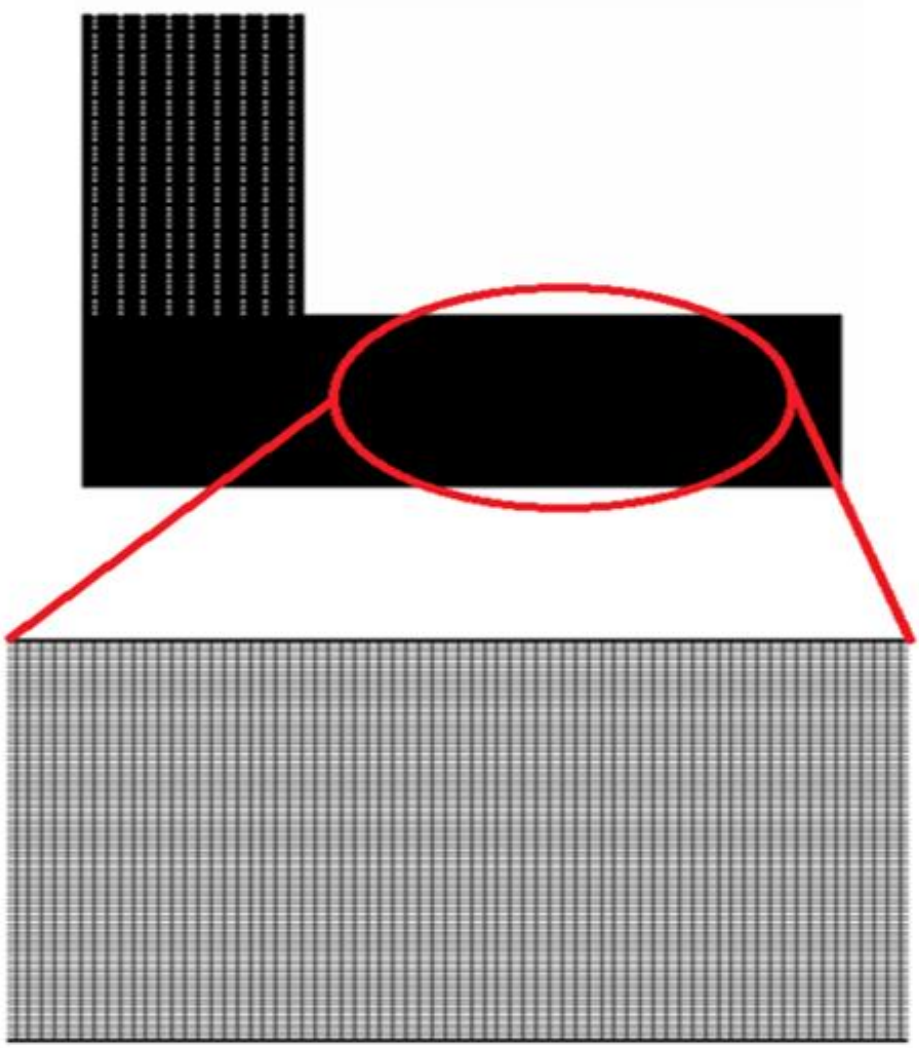

Fig. 4.4: Blown up view of meshed model

For meshing hexahedral elements were used and it can be noticed that there is a very fine uniform mesh for better resolvement of boundary layers and to obtain better accuracy. The mesh quality is presented in Table 1. Grid independence test was carried out for grid sizes of 70, 90, 95 and 100. The quality of mesh measurement method used for the hexahedral elemental was aspect ratio.

In Table 1, different column shows different properties where the aspect ratio of maximum and minimum edge of a cell. The orthogonal quality is exactly one in our meshing and skewness measuring cell shape. The mesh quality is good according to user manual of the software being used.

The grid cross section is as shown in Fig. 4.4 the near wall cell thickness adjacent is sufficient in the entire domain for all cases. The number of cells in the direction normal to the wall is kept constant for the grid independence test. The topology is fully hexahedral in nature with perfect orthogonality with increasing the mesh in the vertical direction only. Impinging jets are very difficult to be modeled in CFD. The flow features of the near wall region makes the wall fluxes difficult to capture with some of the common near wall assumptions already included and fully implemented in the turbulence models themselves.

Chapter 5

Results and Discussion

Present study is on the steady circular hydraulic jump under different flow conditions and measuring the Nusselt number at the stagnation point. The flow structure both upstream of the flow and also the downstream is analysed by a flow over a run-out plate up to a finite distance. Here in this analysis the effect of surface tension is also taken into consideration. This sudden jump in the water depth is contributed to the phenomenon of hydraulic jump. The basic problem in the analysis is the determination of the jump radius and the calculation of the Nusselt number due to the heating of the plate.

There is also an analogous relation between the hydraulic jump and a detonation wave, which is actually a shock wave which is produced by the enormous energy released immediately behind the shock. The flow behind the jump is assumed to be supercritical and after the jump to be subcritical. The fluid thickness is all in the range of only a millimetre.

The 2D axisymmetric simulations were done using transient time steps with a fixed variation. This method uses a pseudo-transient time stepping approach and it allows us to get the solutions faster and robustly.

The plate temperature is maintained below the boiling temperature of water. The heat transfer coefficient and the Nusselt number were calculated for various water speeds in the range 1-5 m/s. The inlet temperature was at 20^{o}C and bottom of the plate was at constant temperature at $100\,^{o}$C.

In the simulations the jet diameter d = 30 mm and placed perpendicular to the heated plate above it at a distance of 250 mm. The radial measurement of plate was 1000 mm. The radial measurement of 1 m was taken to take into account the analysis at higher Reynolds number.

The transient simulations are run at Re = 30000, 60000, 90000, 120000, 150000. The five sets of results are compared with various correlations to evaluate the modeling performed.

Since the current study is a steady state case, all the properties are time averaged with a lesser accuracy requiring higher order discretization schemes for better accuracy to be implemented.

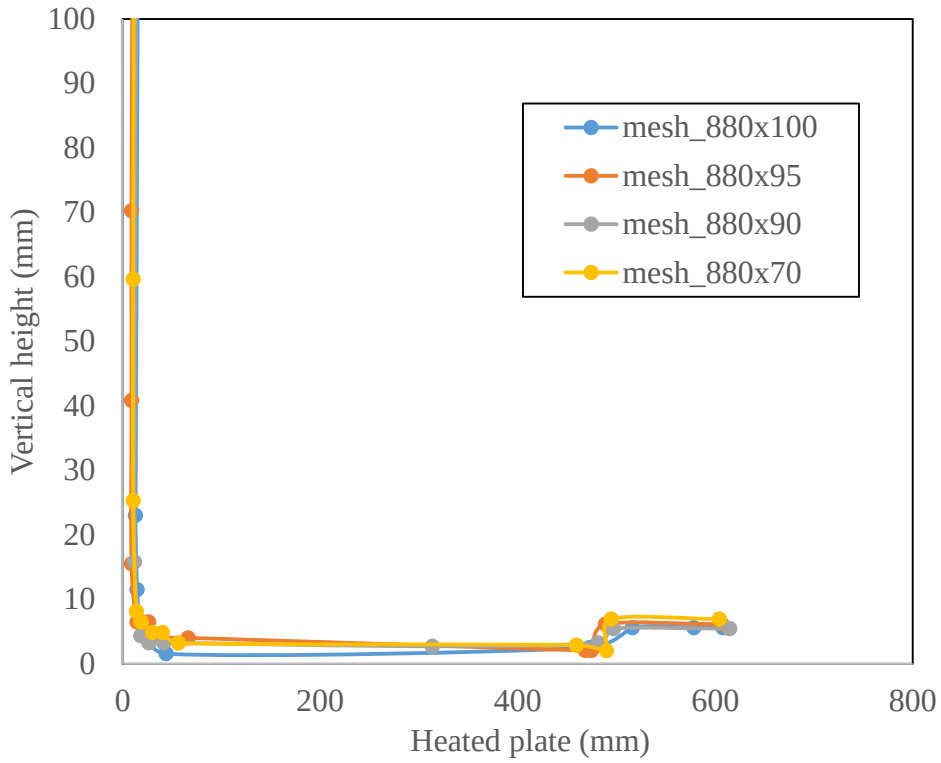

Fig. 5.1: Grid independence test comparison

A grid independence test was conducted for the computational domain under consideration. As an example, for water velocity of 2 m/s in the nozzle, the air water interface for the case of hydraulic jump is predicted at different grid sizes and is reported in Fig. 5.1. Brechet and Neda [15] had presented a correlation to predict the radial distance from the center (i.e. exactly below the center of the nozzle) at which hydraulic jump will appear, is given by,

$$R_{hj} = \left(\frac{27 g^{-1/4}}{2^{1/4} 35 \pi} \right)^{2/3} q^{2/3} d^{-1/6} \nu^{-1/3} \qquad (17)$$

For the grid independence presented in Fig. 5.1, d = 0.03 m and velocity is 2 m/s, for which R_{hj} comes out to be 394 mm. The numerical results presented in Fig. 5.1 predicts the value of R_{hj} = 473 mm. The difference between the two predictions is approximately 20.8%. According to [15] the theoretical results are obtained by considering real, viscous liquids using a scaling law. The experimental results conducted by the authors and the theoretical results predicted were having a difference of 37.5%. Brechet and Neda [15] also reported that experimental values higher than the predicted values using Eq. (17). Similar observation found in the present study. Thus the outcomes

of the present simulation are validated. The numerical prediction is carried out using four different grids 880×70, 880×90, 880×95, 880×100. As shown in the Fig. 5.1, the hydraulic jump showed a higher value of 490 mm for the grid size 880×70. This value improved considerably when the grid size was increased to 880×90 to 481 mm. When the grid size was again increased incrementally to 880×95 the location of the hydraulic jump increased to 475 mm. This grid size was again incrementally increased to 880×100 to which the location of the hydraulic jump remained at 473 mm with negligible changes hence verifying to be grid independent.

The iterative time advancement iterative technique is used currently. The primary fluid used is air and the secondary fluid used is water. So an interface is formed between the primary phase and the secondary phase. The interface is set to a contact angle of 36 degrees. Surface tension coefficient is set to 0.073N/m for the phase water. Wall adhesion is switched off. The flow considered is turbulent in nature and incremental velocities of 1, 2, 3, 4, 5, 6 and 7 m/s are considered for simulation. The lower plate is heated below the boiling point of water at 100 degree Celsius. The x-axis is set as the axis as we are using the axisymmetric condition. Also a parallel solver was used with pressure based solver.

The pressure-velocity coupling used was SIMPLE scheme with presto pressure correction scheme and second order upwind scheme for the purpose of discretization for momentum equations. A first order implicit transient formulation was used. Geometric reconstruction technique for interface was used and implicit body force was considered for body force formulations. The convergence criteria were set as 10^{-6} for continuity and 10^{-8} for energy. The energy equation was implemented in solution since our study involves the analysis of heat transfer.

The global courant number was set to 0.25, the minimum time step size being 10^{-4} and the maximum being 10^{-8}. The maximum iterations per time step was considered as 20.

For the lower wall boundary conditions the plate was set as a stationary wall with a constant wall temperature condition.

The abrupt change in the film thickness is hydraulic jump. These jumps have a characteristic strongly distorted free surface, a boundary layer region and a subsequent separation of flow. Here we show the full domain computational contours of the hydraulic jump radius along with the enlarged zoomed part of the exact radius of hydraulic jump. The change in the sub critical thickness to the supercritical thickness can be easily noticed.

5.1 Effect of acceleration due to gravity on the stagnation zone

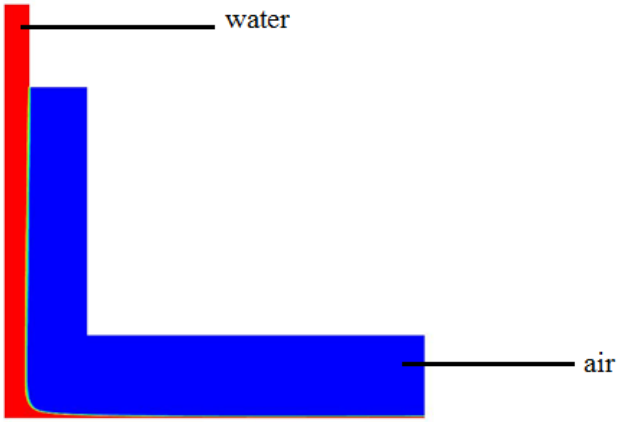

Fig. 5.2: Interface at 1 m/s jet

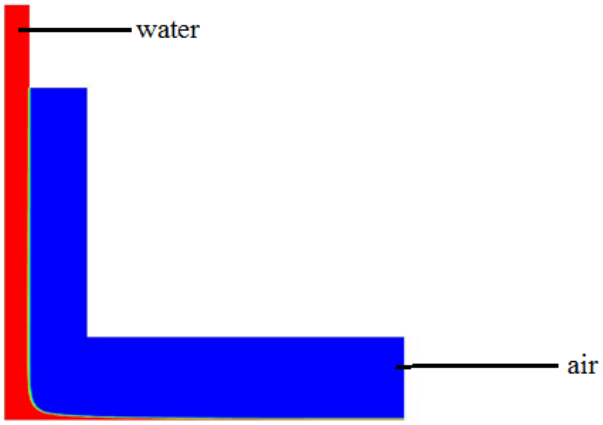

Fig. 5.3: Interface at 3 m/s jet

The VOF method was used to simulate the free surface flow of water as it leaves the nozzle, using the geometric reconstruction for simulations. Fig. 5.2 and 5.3 show the phase contour for water jet leaving the nozzle and strikes the horizontal flat plate for two different nozzle velocities. The jet diameter decreases as it moves downward, may be due to acceleration due to gravity. This can be predicted using the correlation [1] as given below:

$$\frac{d_j}{d} = (1 + 2g(z - z_0)/u_0^2)^{-1/2} \tag{18}$$

Here $d_j(z)$ is the diameter of the water jet as it moves downward, d is the diameter of the nozzle, z_o is the height of the nozzle from the horizontal flat plate, z is the variable which is the distance from the nozzle at which diameter of the water jet desired.

Table 2: Jet diameter for 2 m/s by simulation

d_j(m)	Z_0(m)
0.01462864	0.2007744

0.01192322	0.15700914
0.0114021	0.11160391
0.01141699	0.08425155
0.011023	0.05306896
0.01090183	0.02790538

Table 3: Variation of jet diameter according to Eq. (18)

d (m)	Z(m)	z0(m)	u0(m/s)	d_j(m)
0.03	0.2	0.2	2	0.03
0.03	0.21	0.2	2	0.02929
0.03	0.22	0.2	2	0.02863
0.03	0.23	0.2	2	0.02801
0.03	0.24	0.2	2	0.02743
0.03	0.25	0.2	2	0.02688

Whenever a liquid jet hits a wall surface, sudden increase in pressure occurs which then forces the liquid to accelerate from the stagnation point. Also the one of the efficient ways of obtaining the large heat transfer coefficients are by the impinging jets on a flat surface. The rate of heat transfer is mainly a factor of the jet spacing distance between the nozzle and the target surface, the jet exit velocity and turbulence.

5.2 Phase contours depicting the formation of the radius of hydraulic jump

In fluid single phase simulation, Geoconstruct is used for capturing the free-surface interface. The hydraulic jump radius after reaching the steady state condition continues to remain in that radius until the flow rate changes.

The radius of the circular hydraluic jump depends mainly on the diameter of the nozzle, the distance between nozzle and plate, the surface roughness, fluid properties and the velocity of impingement. The radius of the circular hydraulic jump keeps moving farther away from the centreline of the nozzle as the velocity of jet impinging on the heated plate increases. This aslo depends on the time required for the circular hydraulic jump to become time steady i.e., it doesnot fluctuate with time and remains constant for that particular flow rate condition. As shown in Fig. 5.4 to Fig. 5.9. The location of the full view of the model with the hydralic jump are shown and also an enlarged view is presented.

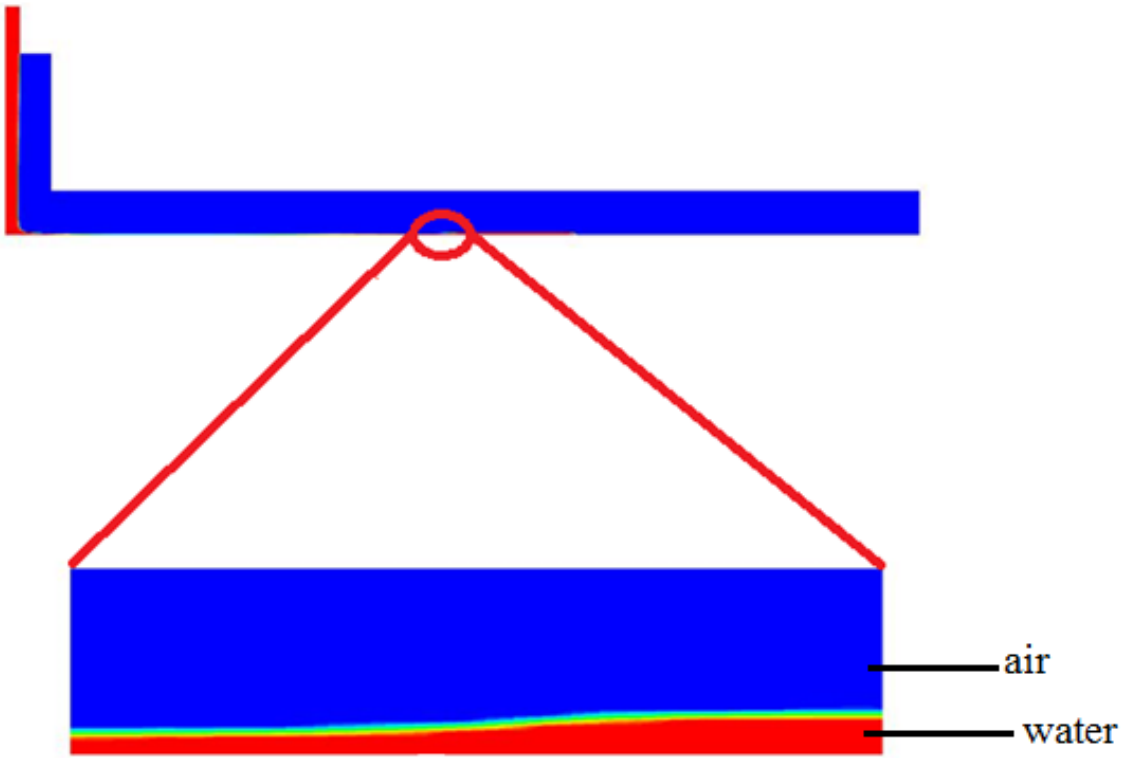

Fig. 5.4: Phase contour view of hydraulic jump at 1m/s and an enlarged view of hydraulic jump.

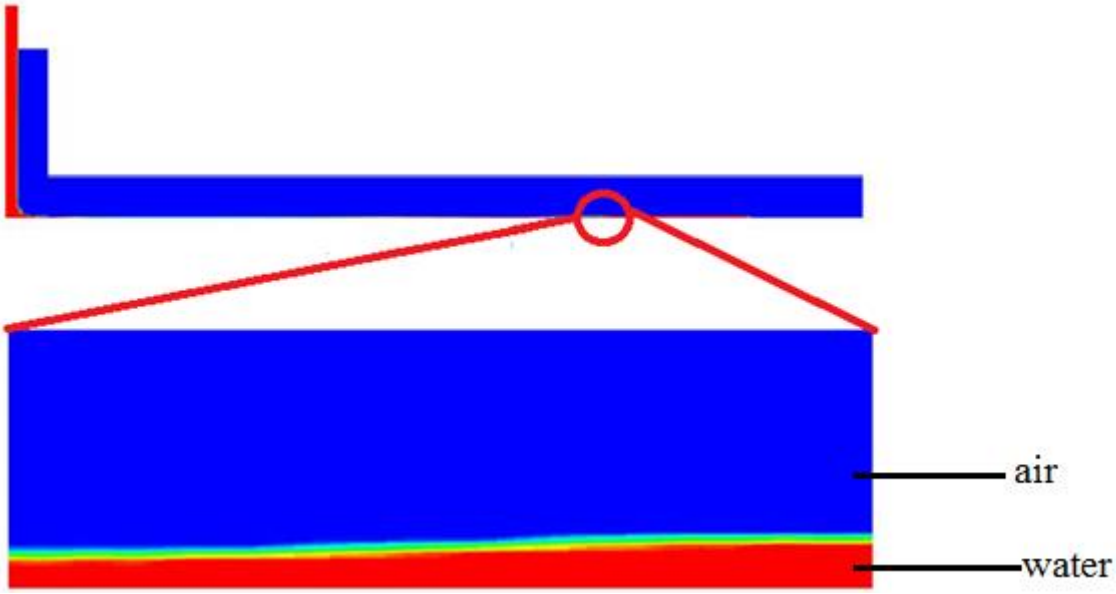

Fig. 5.5: Full hydraulic jump contour view at 2 m/s and an enlarged view of hydraulic jump.

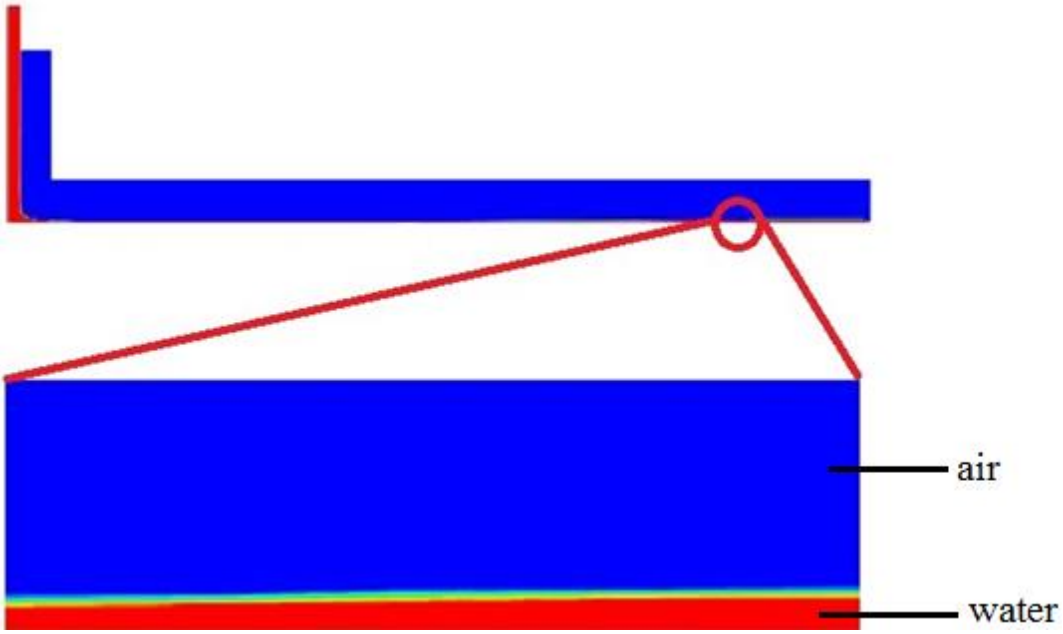

Fig. 5.6: Full hydraulic jump contour view at 3 m/s at t = 1.7sec and an enlarged view of hydraulic jump.

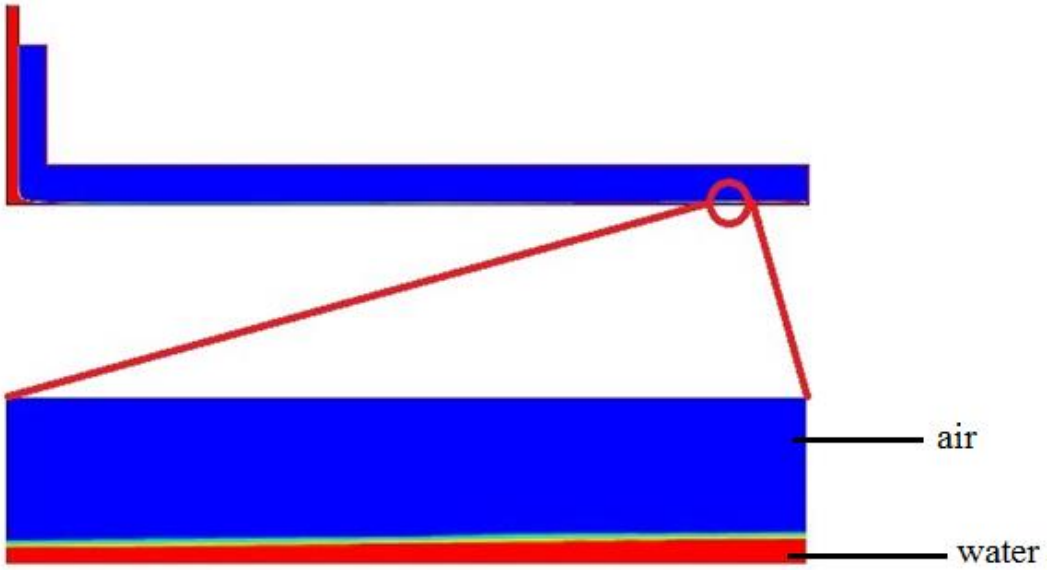

Fig. 5.7: Full hydraulic jump contour view at 4 m/s at t = 1.15 sec and an enlarged view of hydraulic jump.

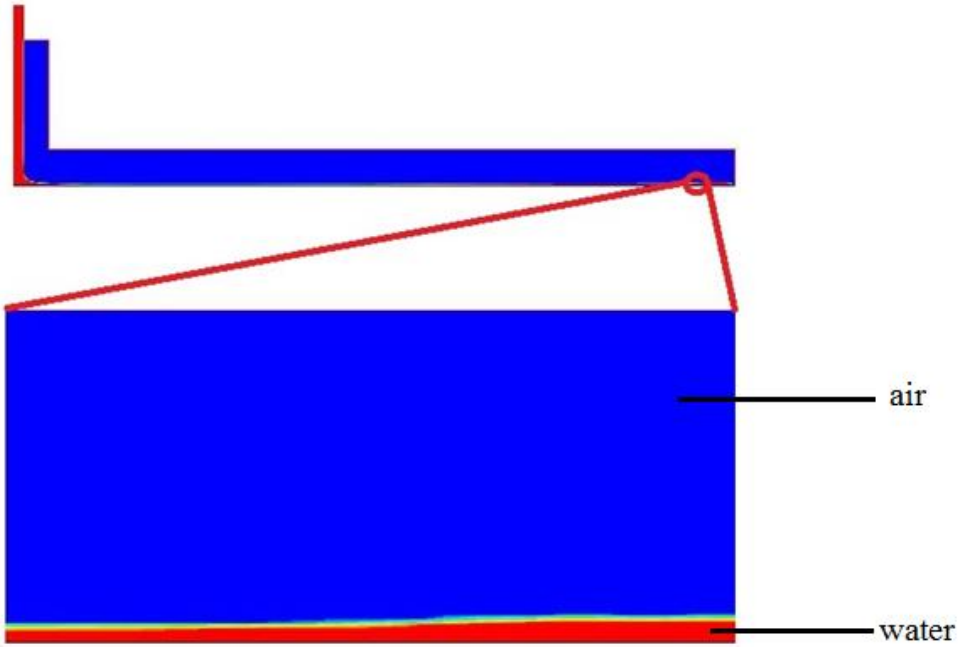

Fig. 5.8: Full hydraulic jump contour view at 5 m/s at time t = 0.9 secs and an enlarged section of hydraulic jump.

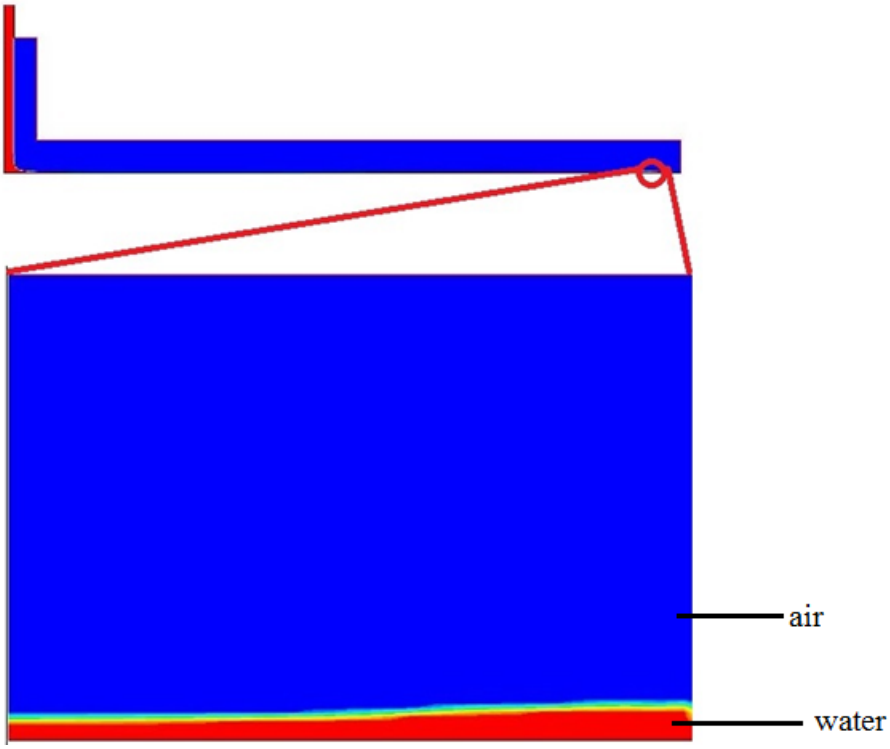

Fig. 5.9: Full hydraulic jump contour view at 6 m/s at time t = 0.65 secs with an enlarged section of hydraulic jump.

5.3 Film thickness

According to the correlation as in Eq. (19) given by Liu et al. [16], the thickness of axisymmetric liquid sheet which varies along the radial direction i.e. h(r) on the surface beginning from the radial position given by:

$$\frac{h(r)}{d} = \frac{0.1713}{(r/d)} + \frac{5.1417}{\mathrm{Re}_d}\left(\frac{r}{d}\right)^2 \tag{19}$$

Surface tension is an important criteria for determining the shape of the circular hydraulic jump for impinging jets. This is the result of thinning of liquid film occurring in circular jumps. The instabilities occur as the subcritical liquid film becomes thicker and hence leading to the decrease in the effect of surface tension.

The Geo-construct method is used for capturing the fluid interfaces. The hydraulic jump for a stable 2 m/s velocity is shown as the hydraulic jump remains constant after 2 sec up to 3 sec. Hence it is assumed to be a stable hydraulic jump. As the velocities are incremented the hydraulic jump keeps moving further downstream and outside the computational domain designed for analysis. The time taken for stabilizing is generally considered after many iterations which is considerable in this current case study. The hydraulic jump radius does not change after attaining the steady jump condition.

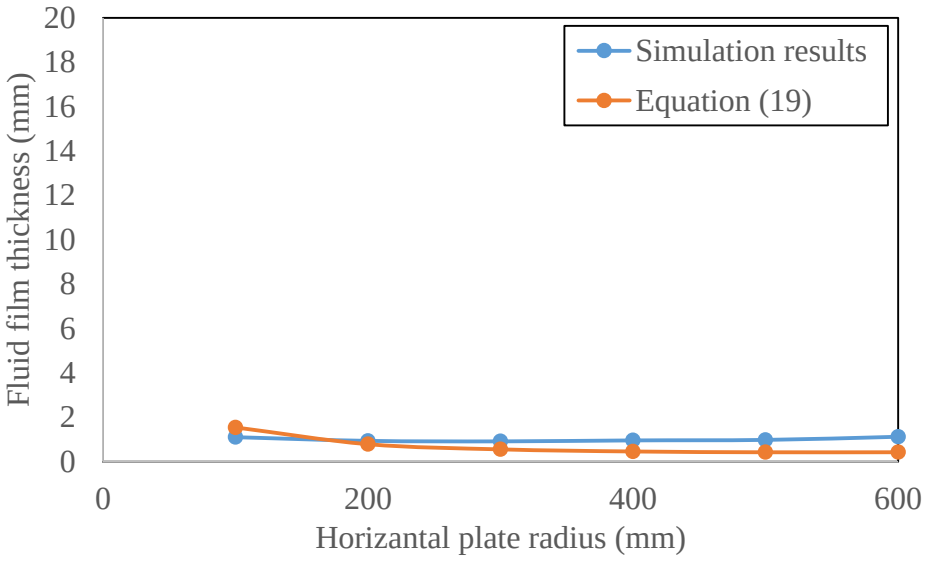

Fig. 5.10(a): Thickness of water varying in radial direction for velocity of water in nozzle = 12 m/s

Eq. (19) is valid for regions outside of the stagnation zone and inside the hydraulic jump radius. By stagnation zone we mean to consider the region almost equal to the diameter of the jet. The correlation does not predict the flow regimes after the super-critical thickness.

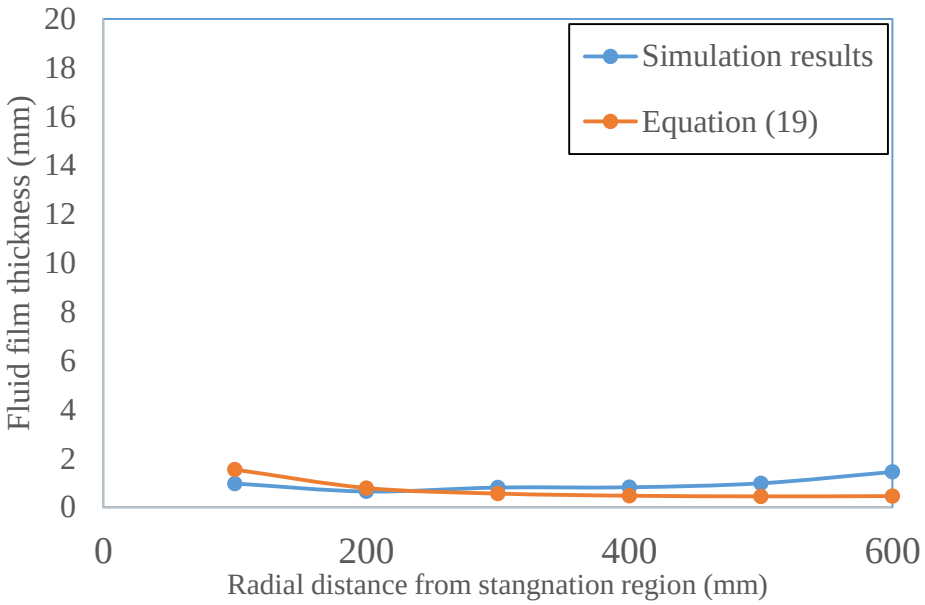

Fig. 5.10(b): Thickness of water varying in radial direction for velocity of water in nozzle = 10 m/s

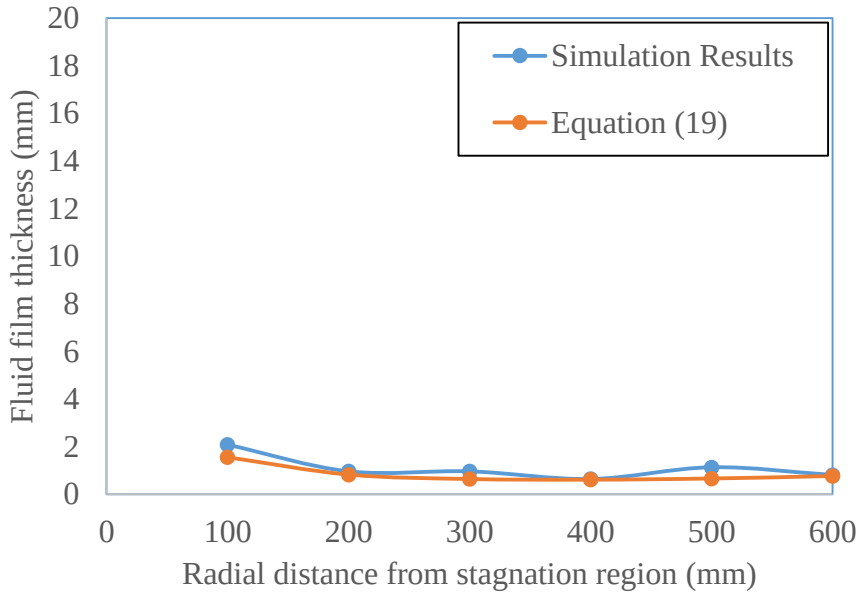

Fig. 5.10(c): Thickness of water varying in radial direction for velocity of water in nozzle = 8 m/s

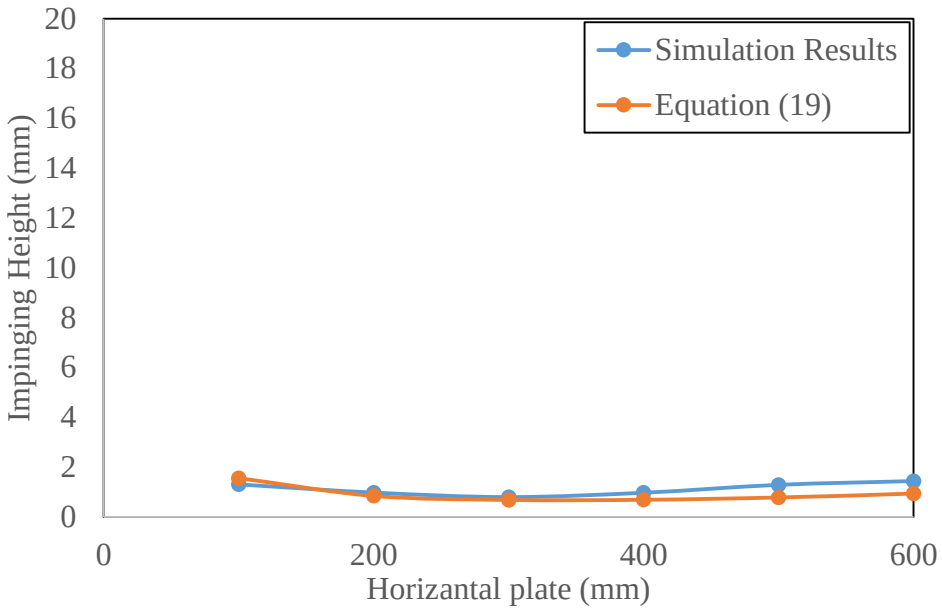

Fig. 5.10(d): Thickness of water varying in radial direction for velocity of water in nozzle = 6 m/s

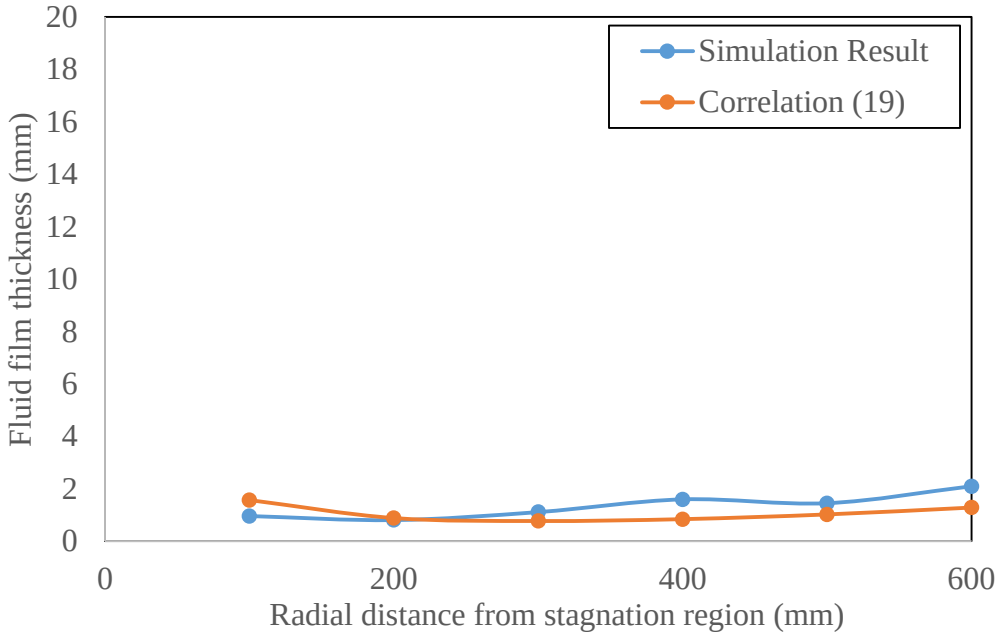

Fig. 5.10(e): Thickness of water varying in radial direction for velocity of water in nozzle = 4 m/s

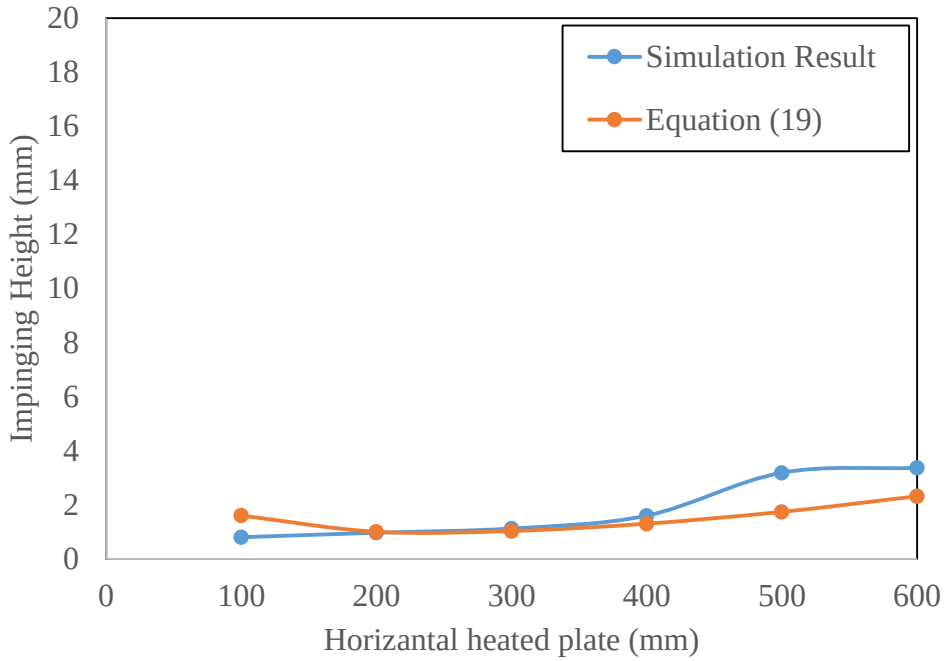

Fig. 5.10(f): Thickness of water varying in radial direction for velocity of water in nozzle = 2 m/s

The thickness of water up to $r < R_{hj}$ is calculated numerically and presented in Fig. 5.10(a-f). The thickness of water predicted using the correlation given in Eq. (19) is also presented in Fig. 5.10(a-f) for direct comparison. It is found that both values are in very good agreement with each other with a maximum deviation of 16% only. It cannot be used to estimate the position of the hydraulic jump but is a very good estimator for the liquid film thickness from the stagnation point before the occurrence of the hydraulic jump.

5.5 Heat transfer under free surface impinging jet – Nusselt Number

Water enters through the inlet at the given velocity and impacts on the heated plate. Due to the high pressure at the stagnation zone it accelerates almost parallel to the plate at sub critical speed.

The plate on which the jet strikes is being maintained such that water will be in liquid phase only. This is done due to the complexity of modelling boiling heat transfers in our investigation. The boundary conditions applied are constant temperature at the plate considering zero wall thickness,

under the assumption that the temperature gradient in the steel thickness of 4 mm is very negligible and hence can be neglected. The plate is hence maintained constantly at 100°C.

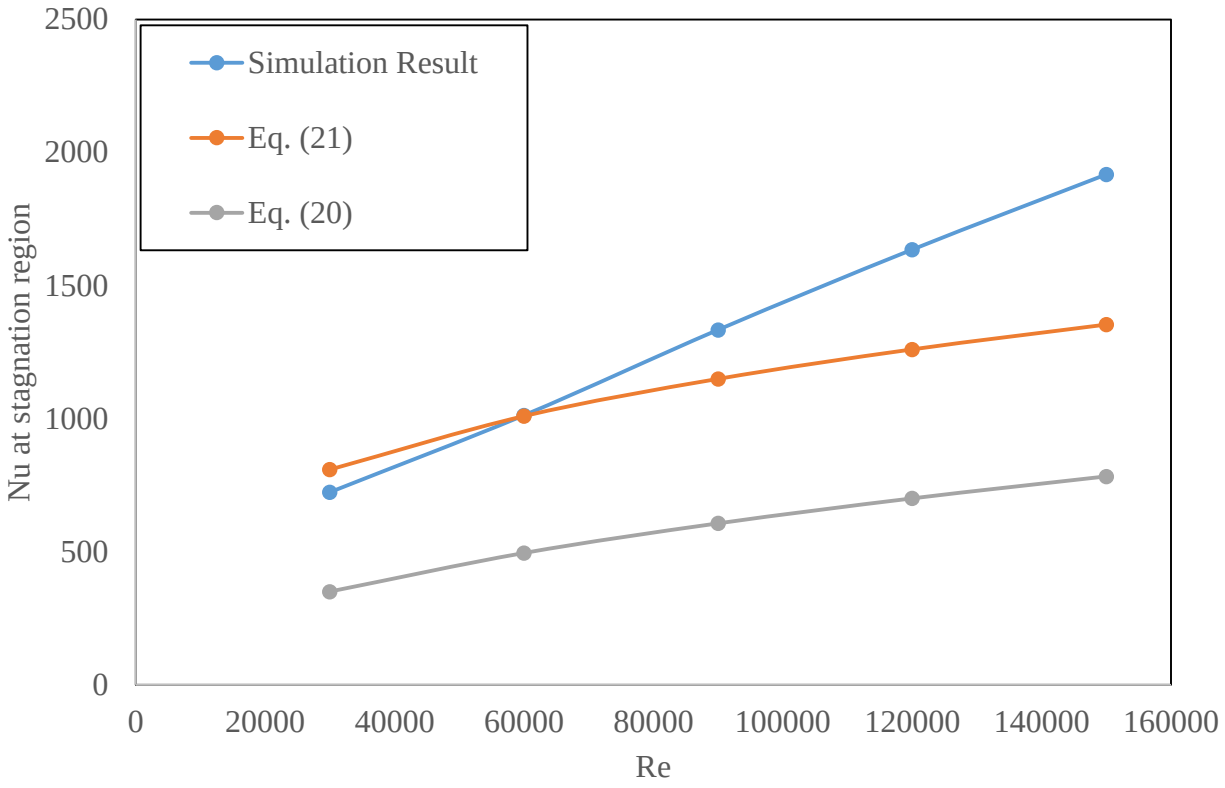

Fig. 5.16: Variation of Nusselt number with Reynolds number

Estimation of the Nusselt number is of paramount importance in this simulation. The heat transfer coefficient is to study the effect of turbulence on the heat transfer between plate and the impacting jet. The impinging jets are correlated in the stagnation region got heat transfer. Here we have compared the nusselt number for different Reynolds number and plotted them against the resulting Nusselt number.

The correlation for stagnation heat transfer for jets impinging according to Liu et al. [16]:

$$Nu_{d,0} = 0.93 * \mathrm{Re}_d^{0.5} * \mathrm{Pr}^{0.4} \quad (20)$$

The correlation for stagnation heat transfer for turbulent jets impinging from circular-type nozzle [17]:

$$Nu_{d,0} = 2.67 * \mathrm{Re}_d^{0.57} \left(\frac{z}{d}\right)^{\left(\frac{-1}{30}\right)} \left(\frac{u_f}{d}\right)^{\left(\frac{-1}{4}\right)} \mathrm{Pr}^{0.4} \quad (21)$$

The Laminar model is observed to be in closest with simulation results by 30%, whereas turbulence model underestimates the experimental data by 60%.

The Thermal boundary layer cannot reach the free surface as the prandtl number for water is 6.97. The Prandtl number obtained thus far is greater than the critical Prandtl number value developed by Liu et al. [16], beyond which the boundary layer does not grow rapidly enough to reach the surface of liquid film.

Analytical value is always higher than the CFD simulation as the analytical expression solves only the radial momentum equation, but the numerical results are dealing with both the radial and axial momentum equation.

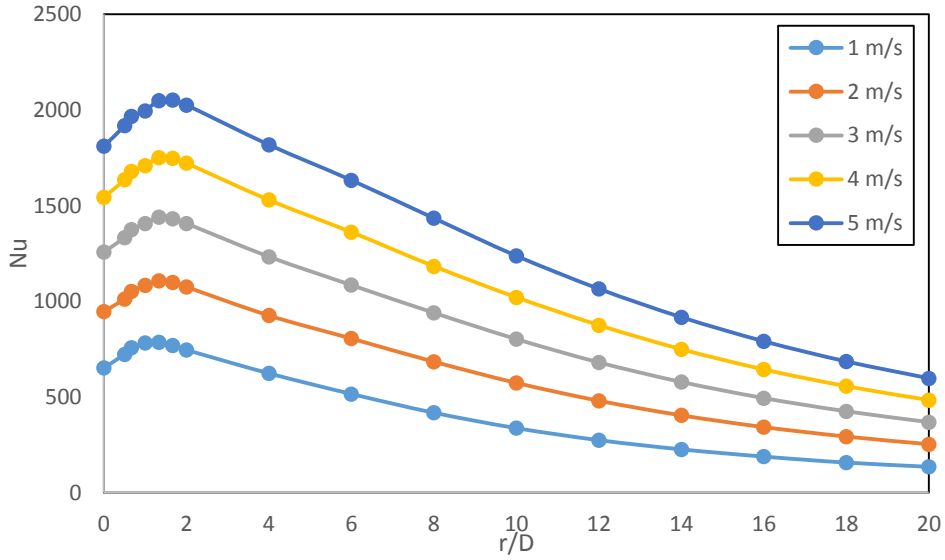

Fig. 5.17: Nusselt number variation with dimensionless radial distance for various Reynolds number

Heat Transfer rates in the stagnation region (0 < d/D < 1.0) show a higher heat transfer coefficient at the stagnation point increasing the removal of higher heat fluxes. For z/D there is no observation of the secondary peak as it is not formed in our investigation.

High heat transfer rate depends strongly on the jet inlet conditions such as the velocity profile, nozzle shapes and diameter, turbulence intensity and the nozzle to plate distance.

Chapter 6

Conclusion and Future work

The objective of this work is to evaluate different approaches to the simulations of impinging jets for a run-out table. Considering turbulence models, k-ε is verified to be not sufficiently accurate in predicting heat transfer and the radius of the hydraulic jump. The V2F model is should be used. With a constant nozzle to wall distance as considered in our case we have validated out simulation of using a less approximate RNG k-ε turbulence model with available fluid flow and heat transfer correlations. They seem to agree well.

Current trend indicates numerical simulations are used to study the effect of heat transfer in the run-out for proper cooling techniques. Hence these simulations will be beneficial to a researcher to know the advantages and disadvantages of using a particular model for such studies.

In our current study analysis we carried out the heat transfer phenomenon of a single phase impinging jet of water on a stationary surface. This study also made an assumption of maintaining the surface below the boiling temperature of water although a very temperature above the boiling point of water is in practical condition on the run-out. Also it must be noted that the surface is not stationary in practice but a continuously moving metal. Hence a study of two phase flow heat transfer and a moving surface condition is to be done in the future.

Another realistic assumption would be to consider the DNS and LES model of turbulence in FLUENT. RNG model is not effective in the prediction of the Nusselt number by overestimating the actual value. But the industrial use is very difficult hence another method of computational resourceful study is necessary. There is a lot of uncertainty in the prediction of the heat transfer coefficient.

The wall thickness considered is negligible here hence for all practical applications a suitable thickness is required to be assumed. When a thickness is present there will be a need to involve conjugate heat transfer phenomenon by considering the axial back conduction factor.

The turbulence model needs to be probed and investigated further to resolve the mesh up to the smallest eddy. Instantaneous velocities should be considered for better accuracy. The correlation for heat transfer for prediction of Nusselt number has to be improved to bring closer the modelled and correlation results.

The inlet velocity profile has a significant influence on the simulation. Uniform velocity profile cannot be used in our studies. The use of finer grids and by using higher numerical discretization provides a non-axisymmetric solution but agrees with experimental data. The relative low nature of convergence is mainly attributed to the cyclic oscillation of the residuals.

References:

1. Hosain, M. L., 2013, CFD Simulation of jet cooling and implementation of flow solvers in GPU, Master's Thesis, Royal Institute of Technology, Stockholm, Sweden.
2. Hallqvist, T., 2006, Large eddy simulation of impinging jet with heat transfer, Technical report, Royal Institute of Technology –Mechanics, Stockholm, Sweden.
3. Lienhard, V. J. H., 2006, Heat transfer by impingement of circular free-surface liquid jets, 18th National & 7th ISHMT-ASME Heat and Mass Transfer Conference, January 4-6, 2006.
4. Arakeri, J. H., Rao, K. P. A., 1996, On radial film flow on a horizontal surface and the circular hydraulic jump, Journal of Indian Institute of Science, 76(1), pp. 73-91.
5. Henningson, D., Berggren, M., 2005, Fluid dynamics: Theory and computation, KTH-Mechanics, Royal Institute of Technology, Stockholm, Sweden.
6. FLUENT® theory guide and user manual, ANSYS FLUENT® 14.5.
7. Hirt, C. W., Nicholas, B. D., 1982. Volume of Fluid (VOF) method for the dynamics of free boundaries, Journal of Computational Physics, 39, pp.201-1225
8. Fujimoto H., Hatta N., Viskanta R., 1999, Numerical simulation of convective heat transfer to a radial free surface jet impinging on a hot solid, Heat and Mass Transfer, 35(4), pp. 266-272.
9. Craik, A. D. D., Latham, R. C., Fawkes M. J., Gribbon, P. W. F., 1981, The circular jump, Journal of Fluid Mechanics, 112, pp. 347-362.
10. Zuckerman, N., Lior, N., 2006, Jet impingement heat transfer: Physics, correlations and numerical modeling, Advances in Heat Transfer, 39, pp. 565-631.
11. Fard, P., Teymourtash, A. R., Khavari, Md., 2013, Numerical study of circular hydraulic jump using volume of fluid method, Journal of Fluids Engineering, 133, pp. 011401-1.
12. Kasimov, A. R., 2008, A Stationary Circular Hydraulic jump, the limits of its existence and its Gas Dynamic Analogue, Journal of Fluid Mechanics, 601, pp.189-198.
13. Bush, J. W. M., Aristoff, J. M., Hosoi, A. E., An experimental investigation of the stability of the circular hydraulic jump, Journal of Fluid Mechanics, 558, pp. 33-52.
14. Kate, R. P, Das, P. K. and Chakraborty, S, An investigation on non-circular hydraulic jumps formed due to obliquely impinging circular liquid jets, Experimental Thermal and Fluid Science, 32, pp.1429-1439.

15. Brechet, Y., Neda, Z., 1998, On the circular hydraulic jump, American Journal of Physics, 67(8), pp. 723-731.
16. Liu, X., Lienhard, V. J. H., Lombara, J. S., 1991, Convective heat transfer by impingement of circular liquid jets, Journal of Heat Transfer, 113, pp. 571-582.
17. Stevens, J., Pan, Y., Webb, B.W., 1992, Effect of nozzle configuration on transport in the stagnation zone of axisymmetric, impinging free surface liquid jets: Part 1- Turbulent flow structure, Journal of Heat Transfer, 114, pp.874-879.